

Synthesis of Silver Nanoparticles Using Phytochemicals of *Azadirachta indica* as Reducing and Stabilizing Agents: Characterization and Antibacterial, Antifungal, Antiparasitic Applications and Biocompatibility Assessment

Sana Habib

Govt. Girls' Degree College Takht Bhai, Mardan, KPK, Pakistan

Muhammad Usman Tariq

Dalian University of Technology, China

Hidayat Ullah Farooqi

Department of Chemistry, University of Swabi, KPK, Pakistan

Nasreen Ashraf*

Government Girls Degree College No. 1 Dera Ismail Khan (affiliated with Gomal University), KPK, Pakistan.

Email: nasreenashraf.714@gmail.com

Muhammad Sabir Hussain*

Department of Botany, Government Degree College No. 1, Dera Ismail Khan (affiliated with Gomal University), KPK, Pakistan

Email: muhammadsabirh118@gmail.com

Author Details

Keywords:

Silver Nanoparticles (AgNPs),
Biofabricated, *Azadirachta indica*,
Phytochemical Analysis,
Antimicrobial Potential,
Antiparasitic Potential

Received on 12 April, 2026

Accepted on 23 May, 2026

Published on 22 June, 2026

Corresponding E-mails &
Authors*:

Nasreen Ashraf

nasreenashraf.714@gmail.com

Muhammad Sabir Hussain*

muhammadsabirh118@gmail.com

Abstract

The present study reports the green synthesis of silver nanoparticles (AgNPs) using aqueous leaf extract of *Azadirachta indica* (Neem) as a natural reducing and stabilizing agent. The phytochemical-rich extract facilitated the conversion of Ag⁺ ions from silver nitrate (AgNO₃) into stable AgNPs under mild conditions, confirmed by a visible color change from pale yellow to dark brown and further validated through UV-Visible spectroscopy showing a characteristic surface plasmon resonance band around 440 nm. The synthesized nanoparticles were systematically characterized using FTIR, XRD, and SEM analyses, which confirmed the involvement of phytochemicals in reduction

and capping, the crystalline nature, and the predominantly spherical morphology of AgNPs. Biological evaluation demonstrated strong, concentration-dependent antibacterial activity against both Gram-positive and Gram-negative bacteria, with notable efficacy against *Pseudomonas aeruginosa* and *Staphylococcus aureus*. Significant antifungal activity was observed against *Candida albicans*, *Aspergillus niger*, and related fungal strains. In addition, the AgNPs exhibited promising antiparasitic activity against selected protozoan parasites, showing increased inhibition with rising nanoparticle concentration. Biocompatibility assessment revealed acceptable cytotoxicity levels and low hemolysis at lower concentrations, indicating a favorable safety profile for biomedical applications. Overall, the study highlights that *Azadirachta indica*-mediated AgNPs possess multifunctional biological activities along with good biocompatibility, making them potential candidates for future antimicrobial and therapeutic applications.

1. INTRODUCTION

Nanotechnology has emerged as a transformative field in modern science, offering innovative solutions across medicine, agriculture, environmental remediation, and industrial biotechnology (Malik et al., 2023). By manipulating materials at the nanoscale (1–100 nm), it is possible to obtain novel physicochemical properties that are not observed in bulk materials. These include enhanced surface reactivity, quantum confinement effects, improved optical behavior, and increased biological interactions. Among various nanomaterials, silver nanoparticles (AgNPs) are of particular interest due to their unique antimicrobial, catalytic, and optical properties (Bamal et al., 2021). Owing to their strong broad-spectrum biological activity, AgNPs have been extensively explored for biomedical applications, particularly as antibacterial, antifungal, and antiparasitic agents (Burduşel et al., 2018).

Conventional methods for nanoparticle synthesis, including chemical reduction, photochemical processes, and physical vapor deposition, often involve hazardous chemicals, high energy requirements, and costly procedures (Jain et al., 2024). Moreover, these methods may produce toxic by-products that limit their biomedical applicability and raise environmental concerns. In

response to these challenges, green synthesis approaches have gained significant attention as sustainable alternatives. Green nanotechnology utilizes biological resources such as plant extracts, bacteria, fungi, and algae to synthesize nanoparticles in an eco-friendly manner (Salem et al., 2013). Among these, plant-mediated synthesis is considered the most efficient and convenient approach due to its simplicity, cost-effectiveness, scalability, and absence of complex maintenance requirements (Mutukwa et al., 2024).

Plant extracts are rich sources of diverse phytochemicals, including flavonoids, phenolic compounds, alkaloids, terpenoids, tannins, saponins, and glycosides (Alamgir et al., 2017). These biomolecules play a crucial role in nanoparticle synthesis by acting as natural reducing, stabilizing, and capping agents. They facilitate the conversion of metal ions into stable nanoparticles while preventing aggregation and controlling particle size and morphology (Manojkumar et al., 2016). Additionally, the biological origin of these capping agents often enhances the therapeutic potential of the synthesized nanoparticles. This synergy between phytochemistry and nanotechnology has opened new avenues for developing environmentally friendly antimicrobial agents. Among medicinal plants, *Azadirachta indica* (Neem) has received considerable attention due to its rich phytochemical composition and well-documented pharmacological properties (Mshelmbula et al., 2023). Neem is widely distributed in tropical and subtropical regions and has been traditionally used in herbal medicine for treating various diseases (Alzohairy et al., 2016). Its leaves contain a variety of bioactive compounds such as nimbin, nimbidin, azadirachtin, quercetin, and other polyphenolic substances. These compounds exhibit strong antioxidant, antimicrobial, anti-inflammatory, and antiparasitic activities, making Neem an ideal candidate for the green synthesis of nanoparticles. The presence of such functional biomolecules enables efficient reduction of silver ions and stabilization of formed nanoparticles, resulting in stable and bioactive nanostructures (Roy et al 2019).

In the green synthesis of silver nanoparticles, silver nitrate (AgNO_3) serves as the precursor source of silver ions (Ag^+), which are reduced to elemental silver (Ag^0) by phytochemicals present in the

plant extract (Melkamu et al., 2021). The reaction typically occurs under mild conditions, and the formation of AgNPs is indicated by a characteristic color change from pale yellow to dark brown due to surface plasmon resonance (SPR). The phytochemicals not only reduce the metal ions but also bind to the nanoparticle surface, preventing aggregation and enhancing colloidal stability (Zuhrotun et al., 2023). The properties of the synthesized nanoparticles can be influenced by several factors, including the concentration of precursor, the amount of plant extract, the temperature, pH, and reaction time (Kaur et al., 2024). Characterization of synthesized nanoparticles is essential to confirm their formation and to understand their physicochemical properties (Joudeh et al., 2022). UV-Visible spectroscopy is commonly used to monitor nanoparticle formation by detecting the SPR absorption band. Fourier-transform infrared (FTIR) spectroscopy identifies functional groups involved in reduction and stabilization processes. X-ray diffraction (XRD) provides information regarding crystalline structure and phase purity, while scanning electron microscopy (SEM) and transmission electron microscopy (TEM) are used to analyze particle size, shape, and morphology. Together, these techniques provide a comprehensive understanding of the structural, optical, and surface properties of the synthesized AgNPs.

AgNPs synthesized through green routes have demonstrated significant biological activities, particularly in antimicrobial applications (Patel et al., 2023). Their antibacterial effects are mediated through multiple mechanisms, including disruption of bacterial cell membranes, generation of reactive oxygen species (ROS), interaction with DNA, and inhibition of essential enzymes (Vanlalveni et al., 2022). They are effective against both Gram-positive and Gram-negative bacteria, including multidrug-resistant strains. Their antifungal activity is associated with inhibition of hyphal growth, membrane disruption, and interference with ergosterol biosynthesis. Furthermore, AgNPs exhibit antiparasitic activity by inducing oxidative stress, disrupting membrane integrity, and impairing metabolic functions in parasites. The synergistic interaction between AgNPs and phytochemicals from *A. indica* further enhances their overall therapeutic potential. The integration

of plant-based synthesis with nanotechnology provides a sustainable platform for developing novel antimicrobial agents. In this context, *Azadirachta indica*-mediated synthesis of AgNPs offers a promising approach for producing environmentally benign nanomaterials with enhanced biological activity (Mohan et al., 2025). This method not only reduces reliance on toxic chemicals but also improves the biocompatibility and efficacy of the nanoparticles, making them suitable for biomedical and environmental applications.

This study aims to synthesize AgNPs using *Azadirachta indica* leaf extract as a natural reducing and stabilizing agent and to evaluate their physicochemical characteristics and biological activities. The specific objectives include the preparation of aqueous leaf extract of *A. indica* and its qualitative phytochemical analysis, green synthesis of AgNPs using silver nitrate (AgNO_3) under optimized conditions, and assessment of key synthesis parameters such as extract concentration, reaction time, and temperature. Furthermore, the study aims to characterize the synthesized nanoparticles using UV-Visible spectroscopy, Fourier-transform infrared (FTIR) spectroscopy, X-ray diffraction (XRD), and electron microscopy techniques to confirm their formation, structural properties, and morphology. In addition, the antibacterial, antifungal, and antiparasitic activities of the synthesized AgNPs will be evaluated against selected pathogenic organisms, while also exploring the role of plant-derived phytochemicals in the reduction of silver ions and stabilization of nanoparticles, thereby enhancing their overall biological efficacy.

2. Materials and methods

2.1. Chemicals and apparatus

All reagents used in this study were of analytical grade and were obtained from reputable suppliers, including Merck and Fluka, without further purification. Deionized water was used throughout the experimental work for the preparation of all solutions to ensure reagent purity and minimize contamination. The chemicals employed for the synthesis of AgNPs included silver nitrate (AgNO_3), methanol (CH_3OH), and sodium hydroxide (NaOH). The apparatus and materials used during the experimental procedures comprised Petri plates, test tubes, Whatman No. 1 filter

paper, beakers, volumetric flasks, measuring cylinders, and a magnetic stirrer. For nanoparticle characterization, various analytical instruments, including a UV-Visible spectrophotometer, Fourier-transform infrared (FTIR) spectrometer, X-ray diffractometer (XRD), and scanning electron microscope (SEM), were utilized to investigate the optical properties, functional groups, crystalline structure, and morphology of the synthesized AgNPs.

2.2. Plant Collection and Extract Preparation

Fresh leaves of *Azadirachta indica* were collected from healthy plants in the Rawalpindi region and authenticated before use. The plant material was thoroughly washed with tap water followed by deionized water to remove dust and surface impurities (Tashi et al., 2016). The cleaned leaves were shade-dried at room temperature until a constant weight was achieved and then ground into a fine powder using a mechanical grinder. For extract preparation, a measured amount of the powdered leaf material was boiled in deionized water at 60–80 °C for 20–30 minutes under continuous stirring to facilitate the release of bioactive phytochemicals. The resulting mixture was cooled to room temperature and filtered through Whatman No. 1 filter paper to obtain a clear aqueous extract, which was subsequently stored at 4 °C and used as a reducing and stabilizing agent for the green synthesis of nanoparticles.

2.3. Phytochemical Analysis

The qualitative phytochemical analysis of *Azadirachta indica* leaf extract was carried out using standard preliminary screening methods to identify the presence of major secondary metabolites (Kumar et al., 2018). The aqueous leaf extract was prepared as previously described and used as the test sample. Alkaloids were detected using Mayer's and Wagner's reagents, where the formation of a cream or reddish-brown precipitate indicated a positive result. Flavonoids were identified by the addition of dilute sodium hydroxide solution followed by acidification, producing a yellow coloration that disappeared upon acid addition. Phenolic compounds and tannins were confirmed using ferric chloride solution, which produced a dark green or bluish-black coloration. Saponins were detected through the froth test, in which persistent foam formation indicated their

presence. Terpenoids were identified using the Salkowski test, characterized by the formation of a reddish-brown interface upon treatment with chloroform and concentrated sulfuric acid. Glycosides were screened using the Keller–Killiani test, indicated by the development of a brown ring at the interface. All tests were performed in triplicate to ensure reliability and reproducibility of the results.

2.4. Nanoparticles synthesis

AgNPs were synthesized using a green synthesis approach employing *Azadirachta indica* leaf extract as a reducing and stabilizing agent following a previous standard protocol (Poopathi et al., 2015). In a typical procedure, a 1 mM aqueous solution of silver nitrate (AgNO_3) was prepared as the metal precursor. Separately, Neem leaf extract was prepared and filtered as described earlier. For nanoparticle synthesis, 10 mL of plant extract was added dropwise to 90 mL of AgNO_3 solution under continuous magnetic stirring at room temperature. The reaction mixture was stirred for 2–3 hours to ensure complete reduction of silver ions. A gradual color change from pale yellow to dark brown indicated the formation of AgNPs due to surface plasmon resonance. The phytochemicals present in the extract, particularly flavonoids, phenolics, and terpenoids, acted as reducing agents by converting Ag^+ ions into elemental silver (Ag^0), while simultaneously stabilizing the nanoparticles through capping and preventing aggregation. The resulting colloidal suspension was centrifuged at 10,000 rpm for 10–15 minutes, washed repeatedly with deionized water to remove impurities, and finally dried for further characterization.

2.5. Characterization of the prepared nanoparticles

The synthesized AgNPs were characterized using a range of analytical techniques to evaluate their physicochemical properties (Zhang et al., 2016). Ultraviolet–visible (UV–Vis) spectroscopy was employed to confirm nanoparticle formation through the observation of the characteristic surface plasmon resonance (SPR) band. Fourier-transform infrared (FTIR) spectroscopy was used to identify the functional groups involved in the reduction and stabilization of the nanoparticles. The crystalline nature and phase purity of the AgNPs were determined using X-ray diffraction (XRD)

analysis, while their surface morphology, particle size, and shape were examined by scanning electron microscopy (SEM). These characterization techniques collectively provided comprehensive information regarding the structural, optical, and morphological properties of the synthesized AgNPs.

2.6. Antibacterial Assay

The antibacterial activity of the biosynthesized AgNPs was evaluated against six different bacterial strains, including both Gram-positive and Gram-negative organisms, using an earlier published protocol (Tamboli et al., 2013). The selected Gram-positive bacteria included *Staphylococcus aureus*, *Bacillus subtilis*, and *Streptococcus pneumoniae*, while the Gram-negative bacteria included *Escherichia coli*, *Pseudomonas aeruginosa*, and *Salmonella typhi*. The antibacterial assay was performed using the agar well diffusion method under sterile conditions. Briefly, nutrient agar medium was prepared and sterilized by autoclaving at 121 °C for 15 minutes at 15 psi. The sterilized medium was poured into sterile Petri plates and allowed to solidify. Bacterial inocula were prepared by adjusting the turbidity of each culture to match the 0.5 McFarland standard, ensuring uniform cell density. The standardized bacterial suspensions were then uniformly swabbed onto the surface of the agar plates using sterile cotton swabs to create a lawn culture. Wells of approximately 6 mm diameter were punched into the agar using a sterile cork borer. Different concentrations of AgNPs (25 µL, 50 µL, 75 µL, and 100 µL) were carefully loaded into the wells. A standard antibiotic (such as streptomycin or ampicillin) was used as a positive control, while sterile distilled water or plant extract alone served as a negative control. The plates were then incubated at 37 °C for 24 hours. After incubation, the antibacterial activity was assessed by measuring the diameter of the zone of inhibition (ZOI) around each well in millimeters. All experiments were performed in triplicate to ensure reproducibility, and the mean values were recorded. The antibacterial efficacy of the AgNPs was determined by comparing the ZOI values with those of the standard antibiotic and control samples, indicating the dose-dependent

antimicrobial potential of the synthesized nanoparticles. The antibacterial activity was determined using the following formula:

$$\% \text{Inhibition} = T_i / C_i \times 100 \quad (2)$$

Where T_i = inhibition in the test and C_i = inhibition in the control.

2.7. Antifungal assay

The antifungal activity of the biosynthesized AgNPs prepared using *Azadirachta indica* leaf extract was evaluated against selected fungal strains, including *Aspergillus niger*, *Aspergillus flavus*, *Candida albicans*, *Fusarium oxysporum*, *Penicillium notatum*, and *Trichophyton rubrum* (Ahmed et al., 2013). The antifungal assay was performed using the agar well diffusion method under aseptic conditions. Potato dextrose agar (PDA) medium was prepared, sterilized in an autoclave at 121 °C for 15 minutes at 15 psi, and poured into sterile Petri plates. After solidification, fungal cultures were inoculated onto the surface of the agar plates. Fungal inocula were standardized and uniformly spread using a sterile swab to ensure even growth distribution. Wells of approximately 6 mm diameter were created in the agar using a sterile cork borer.

Different concentrations of AgNPs (25 µL, 50 µL, 75 µL, and 100 µL) were introduced into the wells. A standard antifungal agent such as fluconazole or amphotericin B was used as a positive control, while sterile distilled water or plant extract alone served as a negative control. The inoculated plates were incubated at 28 ± 2 °C for 48–72 hours depending on fungal growth rate. After incubation, antifungal activity was assessed by measuring the zone of inhibition (ZOI) in millimetres around each well. and the antifungal activity was determined through the subsequent formula:

$$\text{Growth Inhibition}\% = \times (C - T) / C \quad (3)$$

Where C means the growth of the fungus in the control plate, and T shows the growth of fungi in an AgNPs-treated plate.

2.8. Antiparasitic assay

The synthesized AgNPs were dispersed in sterile distilled water to obtain a stock solution. From this stock, working concentrations corresponding to 25 μ L, 50 μ L, 75 μ L, and 100 μ L were prepared for antiparasitic evaluation. All solutions were freshly prepared before each assay to ensure stability and activity. The antiparasitic activity was evaluated against protozoan parasites, including *Leishmania major*, *Plasmodium falciparum*, *Trypanosoma cruzi*, *Giardia lamblia*, *Entamoeba histolytica*, and *Toxoplasma gondii*. Parasite strains were maintained under appropriate in vitro culture conditions using standard growth media specific to each organism and incubated at optimal temperature and atmospheric conditions.

The antiparasitic activity of AgNPs was determined using an in vitro viability inhibition assay. Parasite cultures were exposed to different concentrations of AgNPs (25 μ L, 50 μ L, 75 μ L, and 100 μ L). Each treatment was performed in triplicate (n = 3) to ensure reproducibility. The treated parasite cultures were incubated for a defined period under controlled conditions. After incubation, parasite viability was assessed using standard microscopic counting and/or viability-based staining methods (e.g., trypan blue exclusion or equivalent assay depending on parasite type). Metronidazole (10 μ g/mL) was used as a reference antiparasitic drug to compare the efficacy of biosynthesized AgNPs. Control groups included untreated parasite cultures maintained under identical conditions. Percentage inhibition was calculated using the following formula:

$$\% \text{ Inhibition} = 100 \times A_{\text{sample}}/B_{\text{control}} \quad (4)$$

where A_{sample} represents the AgNPs-treated sample absorbance, and B_{control} means the absorbance of the control sample.

2.9. Biocompatibility assay

The biocompatibility of *Azadirachta indica*-mediated AgNPs was evaluated using in vitro cell viability and hemolysis assays (Kummara et al., 2016). For cell viability assessment, mammalian cell lines (e.g., L929 fibroblasts or HeLa cells) were cultured in appropriate growth medium supplemented with fetal bovine serum under standard conditions (37°C, 5% CO₂). Cells were

exposed to different concentrations of AgNPs (25, 50, 75, and 100 μ L) and incubated for a defined period. Cell viability was determined using a standard assay (such as MTT or trypan blue exclusion), and percentage viability was calculated relative to untreated control cells.

For hemocompatibility evaluation, fresh erythrocytes were isolated, washed with phosphate-buffered saline (PBS), and incubated with varying concentrations of AgNPs under physiological conditions. After incubation, samples were centrifuged, and hemoglobin release in the supernatant was measured spectrophotometrically. Distilled water and PBS were used as positive and negative controls, respectively, and percentage hemolysis was calculated.

2.10. Statistical assessment

All experiments were performed in triplicate ($n = 3$), and the results are presented as mean \pm standard deviation (SD) to ensure data reliability and reproducibility. Statistical analysis was carried out using SPSS software (version 16.0) and OriginPro 9.0. One-way analysis of variance (ANOVA) was applied to determine the significance of differences among treated groups at different concentrations of AgNPs and control samples. Post hoc comparisons were carried out where necessary to identify statistically significant variations between groups. A p-value of less than 0.05 ($p < 0.05$) was considered statistically significant throughout the study. Graphical representations were generated to visualize dose-dependent responses in antibacterial, antifungal, antiparasitic, and biocompatibility assays, ensuring clear interpretation of the biological effects of the synthesized AgNPs.

3. Results and Discussions

3.1. Phytochemical Analysis

The qualitative phytochemical analysis of *Azadirachta indica* leaf extract confirmed the presence of all tested major secondary metabolites, including alkaloids, flavonoids, phenolics, tannins, saponins, terpenoids, and glycosides (Table 1). Distinct and characteristic color changes or precipitate formations were observed for each class, validating the successful detection of bioactive compounds. Alkaloids were identified by the formation of cream and reddish-brown

precipitates with Mayer's and Wagner's reagents, respectively. Flavonoids produced a yellow coloration in alkaline conditions that disappeared upon acidification, confirming their presence. Phenolic compounds and tannins exhibited strong dark green to bluish-black coloration upon treatment with ferric chloride, indicating a high abundance of polyphenolic constituents. Saponins were confirmed through stable froth formation, while terpenoids showed a reddish-brown interface in the Salkowski test. Glycosides were detected by the appearance of a characteristic brown ring in the Keller–Killiani test. The consistency of results across replicates confirmed the reliability of the phytochemical profile.

The comprehensive phytochemical profile of *A. indica* leaf extract demonstrates the presence of diverse bioactive secondary metabolites that are well known for their pharmacological and biological significance (Saleem et al., 2018). The detection of alkaloids, flavonoids, phenolics, tannins, saponins, terpenoids, and glycosides suggests that the plant possesses strong medicinal potential and multifunctional biochemical properties. Phenolics and flavonoids are particularly important due to their strong antioxidant activity, which plays a crucial role in reducing silver ions (Ag^+) to silver nanoparticles (Ag^0) during green synthesis. These compounds also act as natural capping agents, enhancing nanoparticle stability and preventing aggregation. Tannins further contribute to metal ion chelation and stabilization of nanoparticles, improving their uniformity and biological performance (Sidhu et al., 2022). Alkaloids are known for their broad-spectrum antimicrobial and antiparasitic activities, which may synergistically enhance the biological efficacy of biosynthesized AgNPs. Similarly, saponins possess membrane-permeabilizing properties that can increase nanoparticle interaction with microbial and parasitic cells, thereby improving therapeutic efficiency (Al-Arnoot et al., 2025). Terpenoids and glycosides also contribute significantly to bioactivity, exhibiting antimicrobial, anti-inflammatory, and cytotoxic properties.

Table 1. Qualitative Phytochemical Analysis of *Azadirachta indica*

Phytochemical Class	Observation	Result
Alkaloids	Cream precipitate / Reddish-brown precipitate	+ (Present)
Flavonoids	Yellow color that disappears on acidification	+ (Present)
Phenolics	Bluish-black / dark green coloration	+ (Present)
Tannins	Dark green/black coloration	+ (Present)
Saponins	Persistent stable foam formation	+ (Present)
Terpenoids	Reddish-brown interface	+ (Present)
Glycosides	Brown ring at the interface	+ (Present)

3.2. Characterization of Bio-fabricated AgNPs

3.2.1. UV-Vis Spectrophotometry of AgNPs

The UV-Visible absorption spectrum of the synthesized AgNPs exhibited a characteristic surface plasmon resonance (SPR) band in the visible region, confirming the successful formation of AgNPs (Figure 1). A distinct absorption peak was observed at approximately 440 nm with a maximum absorbance of about 0.55. The absorbance initially decreased from approximately 0.22 at 300 nm to 0.10 at 330 nm, followed by a sharp increase leading to the SPR peak. Beyond the maximum absorption wavelength, the absorbance gradually declined with increasing wavelength, reaching approximately 0.12 at 600 nm and 0.04 at 800 nm. A slight shoulder was observed in the 580–620 nm region, indicating minor variations in particle size distribution. The presence of a

strong and well-defined SPR band in the range of 420–450 nm is characteristic of AgNPs and provides preliminary evidence of their successful synthesis and stability. The UV–Vis spectrum demonstrated a pronounced SPR absorption band centered at approximately 440 nm, which is attributed to the collective oscillation of conduction electrons on the nanoparticle surface upon interaction with incident light. The observed SPR peak falls within the typical range reported for spherical AgNPs synthesized through biological routes. The slight red shift of the absorption maximum compared with bulk silver may be associated with nanoparticle size, surface-bound phytochemicals acting as capping agents, and changes in the local dielectric environment surrounding the nanoparticles.

The broad nature of the absorption band suggests a moderate distribution of particle sizes, while the absence of additional major peaks indicates minimal impurity formation during synthesis. The small shoulder observed around 600 nm may reflect the presence of a minor fraction of larger particles or slight nanoparticle aggregation (Shripad et al., 2025). However, the dominant peak at 440 nm indicates that the synthesized nanoparticles are predominantly spherical and relatively well dispersed. Furthermore, the gradual decline in absorbance at higher wavelengths suggests good colloidal stability and limited aggregation of the nanoparticles. Similar SPR bands in the range of 420–450 nm has been widely reported for green-synthesized AgNPs, supporting the reliability of the present synthesis approach (Lorent et al., 2024).

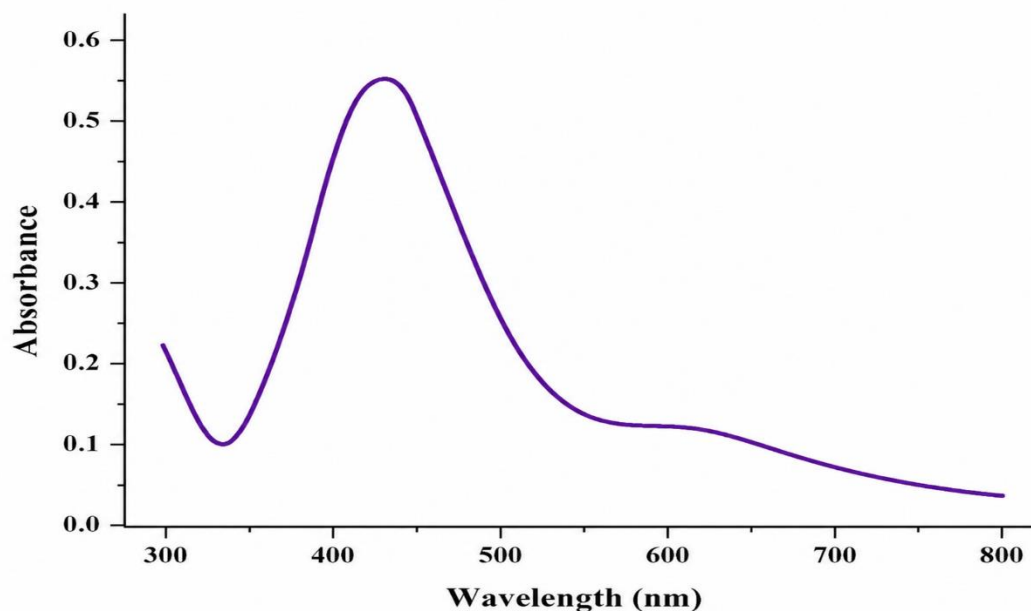


Figure 1. UV spectrum of plant-mediated AgNPs.

3.2.2. XRD study of AgNPs

The XRD was executed to explore the crystalline behavior of the prepared AgNPs (Figure 2). The crystalline properties of the NPs contribute vitally to their performance (Recio-Poo et al., 2023). The plant-mediated NPs proved a crystalline nature and showed characteristic peaks at 2θ . The XRD analysis revealed peaks at 2θ values of 24.2° , 26.3° , 40.2° , and 41.2° , which were indexed to (63), (130), (145), (160), and (165) planes of a cubic structure (Fig. 4), following the JCPD card no. 04-0783. The strongest peak of AgNPs establishes their crystalline nature. The XRD pattern of the AgNPs is aligned with former studies (Hashem et al., 2022). The particle size was calculated as 55 nm. The crystalline sizes of the prepared NPs were calculated with the help of the Debye–Scherrer equation as follows:

$$D = k\lambda/(\beta\cos\theta) \quad (7)$$

where D shows the crystalline size (nm), k is a constant, λ denotes the wavelength of the X-ray radiation, β represents the full width at half maximum (FWHM) of the intensity and broad peaks, and θ is the Bragg's or diffraction angle.

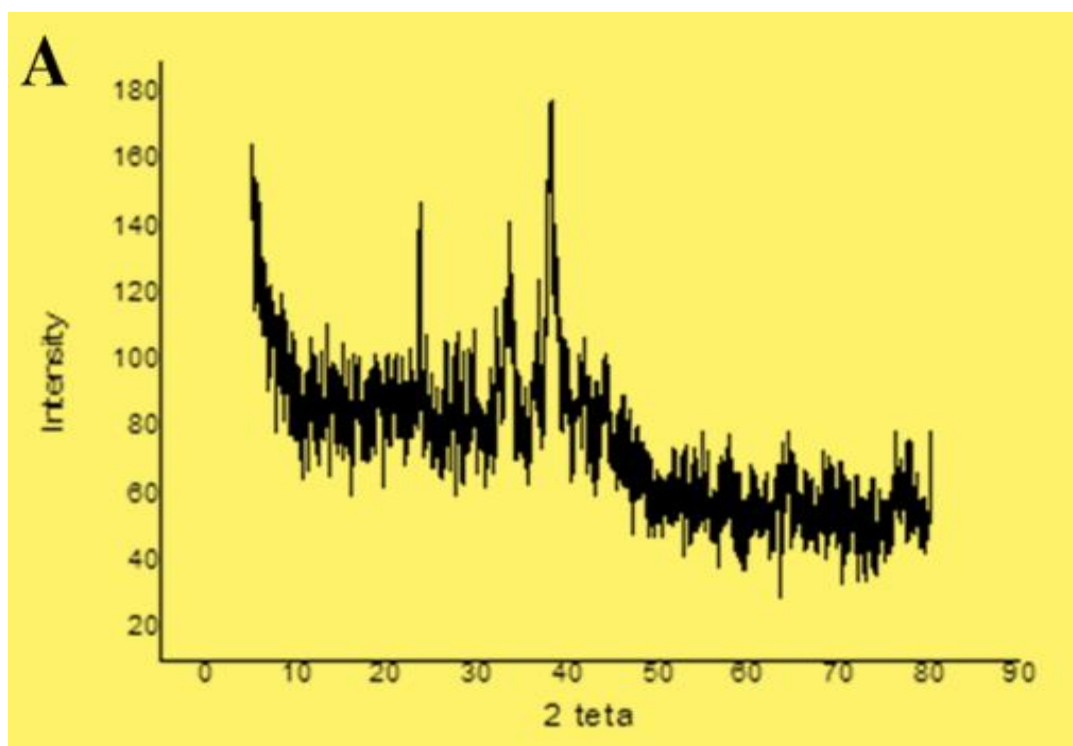


Figure 2. XRD spectrum of AgNPs

3.2.3. FTIR Study

The FTIR spectrum of *Azadirachta indica*-mediated AgNPs exhibited several characteristic absorption bands at approximately 3880, 2790, 2250, 1650, 890, 750, 610, and 500 cm^{-1} , indicating the presence of diverse functional groups responsible for reduction, capping, and stabilization of nanoparticles (Figure 3). A broad absorption band near 3880 cm^{-1} corresponds to O–H stretching vibrations of hydroxyl groups, typically associated with phenolic compounds and adsorbed water molecules. The peak at 2790 cm^{-1} is attributed to C–H stretching vibrations of aliphatic compounds present in plant phytochemicals. The band observed at 2250 cm^{-1} suggests the

presence of $C\equiv N$ (nitrile) or $C\equiv C$ stretching vibrations, indicating involvement of organic biomolecules in nanoparticle stabilization. The prominent peak at 1650 cm^{-1} corresponds to $C=O$ stretching (amide I) or $C=C$ stretching vibrations of aromatic rings, which are commonly associated with proteins and flavonoid structures acting as capping agents. Lower wavenumber peaks at 890 cm^{-1} and 750 cm^{-1} are assigned to $C-H$ out-of-plane bending vibrations of aromatic compounds, confirming the presence of plant-derived phenolics and flavonoids on the nanoparticle surface. The bands at 610 cm^{-1} and 500 cm^{-1} are indicative of metal-oxygen (M-O) or metal-ligand vibrations, which strongly suggest the successful formation of AgNPs and interaction of Ag with phytochemical functional groups.

The FTIR analysis confirms that *Azadirachta indica* leaf extract plays a crucial role not only in the reduction of Ag^+ ions to Ag^0 but also in the stabilization of the synthesized nanoparticles (Chinnasamy et al., 2021). The presence of hydroxyl ($-OH$), carbonyl ($C=O$), and aromatic functional groups indicates that polyphenols, flavonoids, and proteins are actively involved in both reduction and capping processes (Babatimehin et al., 2025). The broad O-H stretching peak suggests strong hydrogen-bonding interactions, which contribute to nanoparticle stability in solution. The amide and carbonyl peaks at 1650 cm^{-1} further confirm the involvement of plant proteins, which may act as natural stabilizing agents by binding to the nanoparticle surface. The appearance of metal-oxygen/metal-ligand vibrations in the low wavenumber region ($500-610\text{ cm}^{-1}$) provides strong evidence for the successful formation of AgNPs (Aljazzar et al., 2026). These interactions indicate that biomolecules from the plant extract remain attached to the nanoparticle surface, forming a protective organic layer that prevents aggregation.

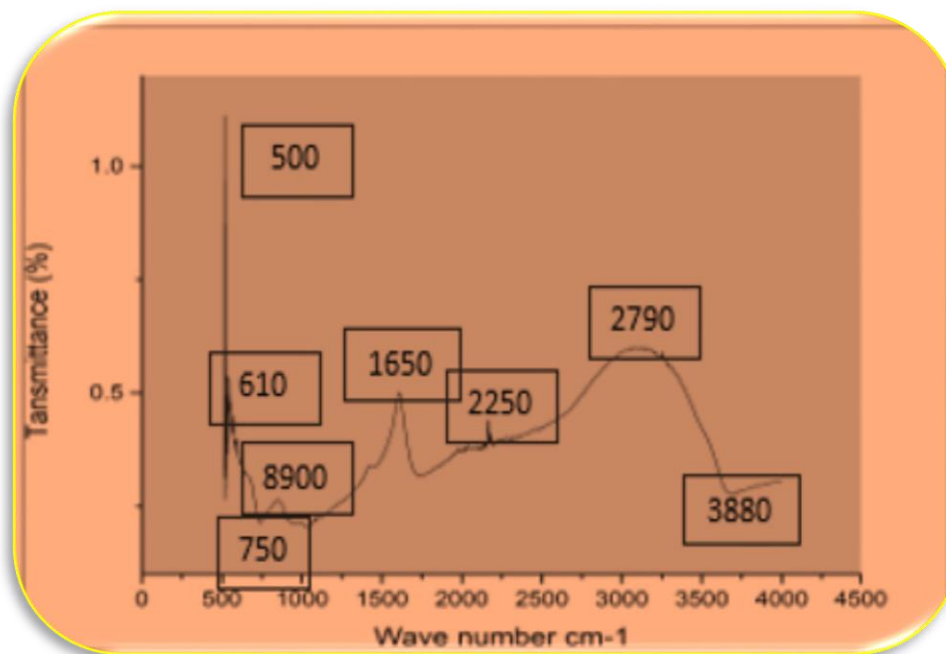


Figure 3. FTIR spectrum of phyto-fabricated AgNPs.

3.2.4. SEM analysis

The scanning electron microscopy (SEM) image of the green-synthesized AgNPs reveals the formation of predominantly spherical to quasi-spherical nanoparticles with a tendency to form agglomerated clusters (Figure 4). The particles are densely packed, indicating strong interparticle interactions, which are commonly observed in biosynthesized nanoparticles due to surface capping by phytochemicals. At higher magnification, the nanoparticles appear to have a rough and slightly porous surface morphology, suggesting that the reduction process mediated by plant extracts leads to heterogeneous nucleation and growth. The particle size distribution appears to be non-uniform, ranging from small nanometer-scale grains to relatively larger aggregated structures. Such aggregation is typical in green synthesis routes where biomolecules act simultaneously as reducing and stabilizing agents but may not provide complete steric stabilization.

The observed morphology can be attributed to the role of phytochemical constituents (such as flavonoids, phenolics, alkaloids, and proteins) present in the plant extract used for synthesis (Kaur et al., 2024). These biomolecules facilitate the reduction of Ag^+ ions to Ag^0 while also capping the nanoparticle surface. However, incomplete or weak capping may lead to agglomeration, as seen in the SEM micrograph. The irregular and clustered morphology may also enhance certain functional properties of AgNPs. For instance, agglomerated structures can increase the effective surface area and active sites, which may improve their antimicrobial and catalytic performance. Similar morphologies have been reported in previous studies on green-synthesized AgNPs, where nanoparticle aggregation was linked to the nature and concentration of the plant extract, reaction temperature, and pH conditions (Jadhav et al., 2024). Furthermore, the absence of well-dispersed individual nanoparticles suggests that optimization of synthesis parameters (such as extract concentration, reaction time, or use of additional stabilizers) could improve uniformity and reduce aggregation.

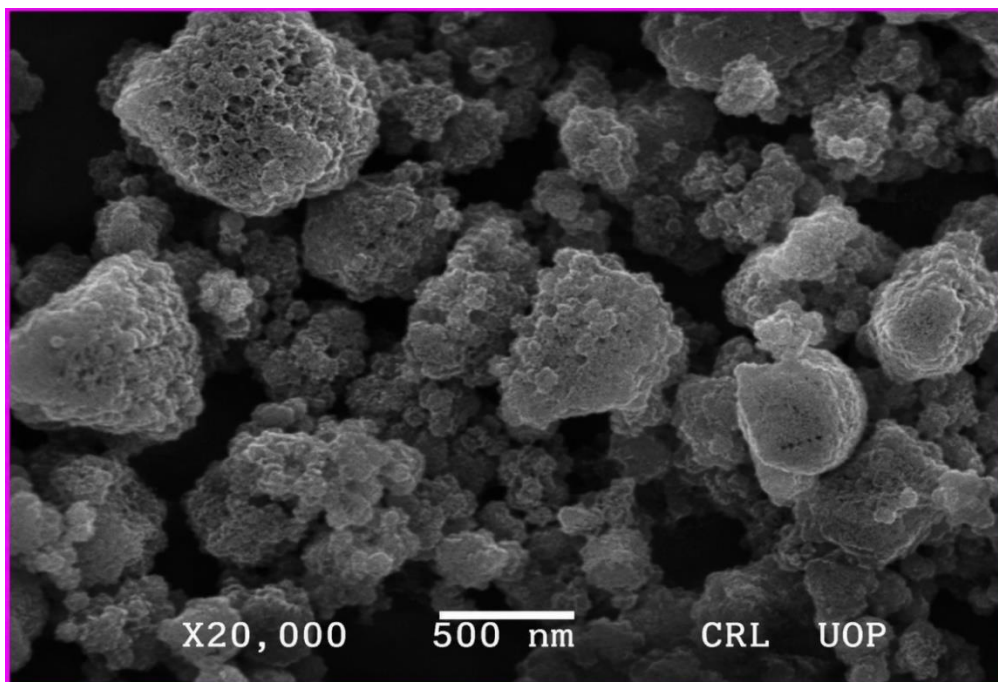


Figure 4. SEM image of bio-fabricated AgNPs

3.3. Antibacterial potential

The antibacterial activity of AgNPs was evaluated against six bacterial strains comprising three Gram-positive (*Staphylococcus aureus*, *Bacillus subtilis*, *Streptococcus pneumoniae*) and three Gram-negative (*Escherichia coli*, *Pseudomonas aeruginosa*, *Salmonella typhi*) bacteria using the agar well diffusion method. The antibacterial effect was determined by measuring the zone of inhibition (ZOI) at different concentrations of AgNPs and compared with a standard antibiotic, streptomycin (10 µg/mL). The results showed a clear concentration-dependent increase in antibacterial activity across all tested bacterial strains. The data presented in Figure 5 demonstrate that AgNPs exhibit significant antibacterial activity against all tested bacterial strains. A clear dose-dependent increase in the zone of inhibition was observed with increasing concentrations of AgNPs from 25 µL to 100 µL. Among the tested organisms, *Pseudomonas aeruginosa* showed the highest sensitivity to AgNPs, with a maximum inhibition zone of 20.6 ± 0.5 mm at 100 µL concentration. This was closely followed by *Staphylococcus aureus* (19.4 ± 0.6 mm), while *Escherichia coli* exhibited comparatively lower sensitivity with a maximum inhibition zone of 15.8 ± 0.4 mm. The standard antibiotic streptomycin (10 µg/mL) showed higher inhibition zones than AgNPs across all bacterial strains, confirming its strong antimicrobial efficacy. However, the AgNPs still demonstrated considerable antibacterial potential, particularly at higher concentrations, indicating their broad-spectrum activity.

The observed antibacterial activity of the biosynthesized AgNPs can be attributed to their small particle size, large surface area, and the presence of bioactive phytochemical capping agents derived from *Azadirachta indica* (Chinnasamy et al., 2021). These nanoparticles interact strongly with bacterial cell membranes, leading to structural damage, increased membrane permeability, and eventual cell death (Ulaeto et al., 2019). Additionally, AgNPs are known to generate reactive oxygen species (ROS), which cause oxidative stress and damage to proteins, lipids, and DNA within bacterial cells. The variation in susceptibility between Gram-positive and Gram-negative bacteria is primarily due to differences in cell wall architecture (Rana et al, 2023) . Gram-negative bacteria

possess an outer membrane composed of lipopolysaccharides, which provides an additional barrier against nanoparticle penetration (Ezeh et al., 2024). However, in this study, *Pseudomonas aeruginosa* still showed high sensitivity, possibly due to enhanced ROS-mediated damage and membrane disruption by AgNPs. Gram-positive bacteria such as *Staphylococcus aureus* and *Bacillus subtilis* also exhibited strong inhibition zones due to their relatively porous peptidoglycan layer, which allows easier interaction with nanoparticles. The slightly lower activity of AgNPs compared to streptomycin is expected, as streptomycin is a purified antibiotic with a specific mechanism of action, whereas AgNPs exert a multi-targeted antimicrobial effect.

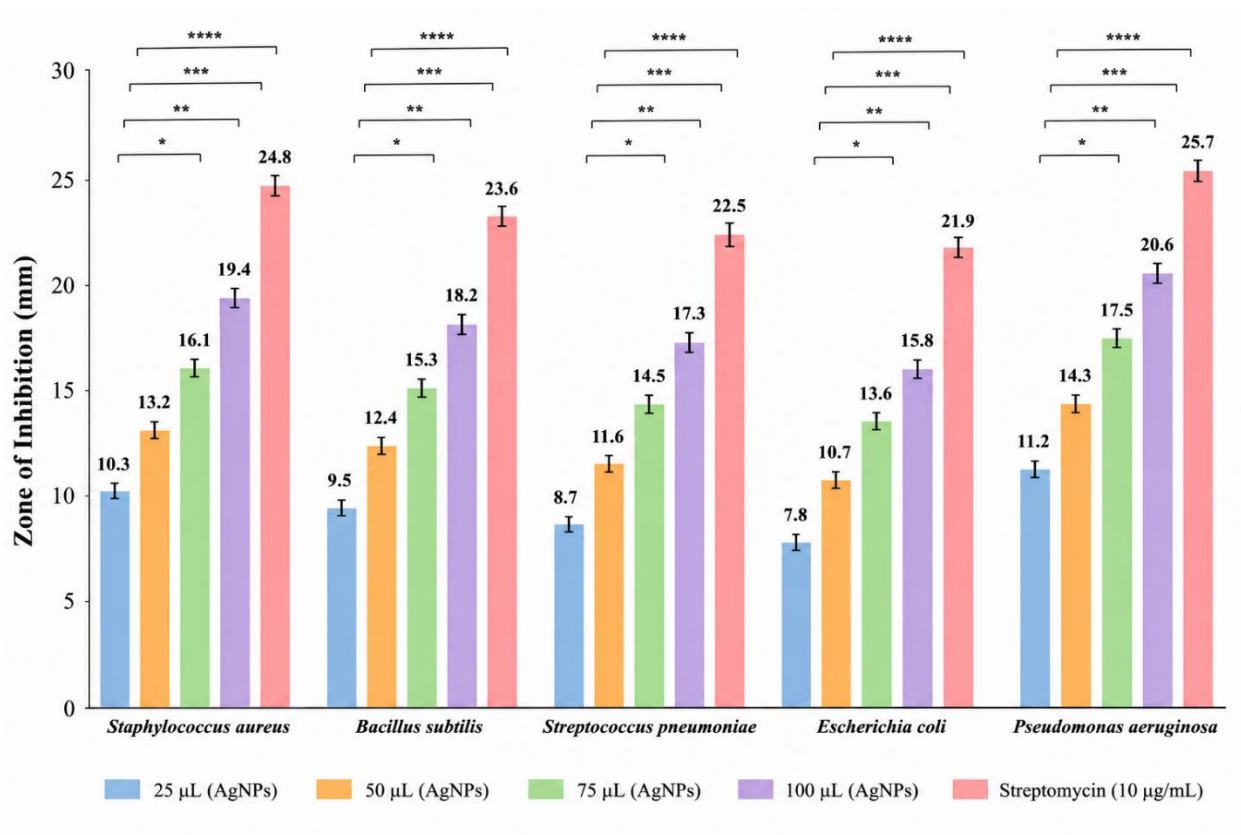


Figure 5. Antibacterial activity of AgNPs synthesized from *Azadirachta indica*

3.4. Antifungal activity

The antifungal activity of AgNPs was evaluated against six fungal strains, including *Aspergillus niger*, *Aspergillus flavus*, *Candida albicans*, *Fusarium oxysporum*, *Penicillium notatum*, and *Trichophyton rubrum*, using the agar well diffusion method. The antifungal effect was assessed by measuring the zone of inhibition (ZOI) at different concentrations of AgNPs and compared with a standard antifungal drug, fluconazole (10 µg/mL). The results revealed a clear concentration-dependent antifungal activity, where inhibition zones increased with increasing AgNP concentration from 25 µL to 100 µL. The results presented in Figure 6 indicate that the biosynthesized AgNPs exhibit significant antifungal activity against all tested fungal strains. A dose-dependent increase in the zone of inhibition was observed with increasing concentrations of AgNPs, confirming enhanced antifungal efficacy at higher doses. Among the tested fungi, *Candida albicans* and *Trichophyton rubrum* showed the highest sensitivity, with maximum inhibition zones of 19.1 ± 0.6 mm and 18.9 ± 0.6 mm, respectively, at 100 µL concentration. In contrast, *Fusarium oxysporum* exhibited relatively lower susceptibility with a maximum inhibition zone of 17.0 ± 0.5 mm. The standard antifungal agent fluconazole (10 µg/mL) showed higher inhibition zones than AgNPs across all fungal strains, indicating its strong specific antifungal activity. However, AgNPs demonstrated substantial antifungal potential, particularly at higher concentrations, suggesting their broad-spectrum inhibitory effect.

The observed antifungal activity of AgNPs can be attributed to their nanoscale size, large surface area, and the presence of bioactive phytochemicals from *Azadirachta indica* acting as capping agents (Ulaeto et al., 2019). These nanoparticles interact with fungal cell membranes, leading to increased permeability, disruption of membrane integrity, and leakage of intracellular components. Additionally, AgNPs induce oxidative stress through the generation of reactive oxygen species (ROS), which damage essential cellular structures such as proteins, lipids, and nucleic acids. The variation in antifungal sensitivity among different fungal strains is likely due to differences in cell wall composition and structural complexity (Giri et al., 2025). Yeast-like fungi

such as *Candida albicans* are more susceptible due to their relatively less rigid cell wall compared to filamentous fungi. On the other hand, fungi such as *Fusarium oxysporum* show moderate resistance due to thicker cell wall structures. Although fluconazole exhibited stronger antifungal activity than AgNPs, the nanoparticles offer a multi-targeted mechanism of action, reducing the likelihood of resistance development. The synergistic effect of silver ions and phytochemicals from *A. indica* further enhances antifungal performance, making these biosynthesized nanoparticles promising candidates for future antifungal therapies and biomedical applications.

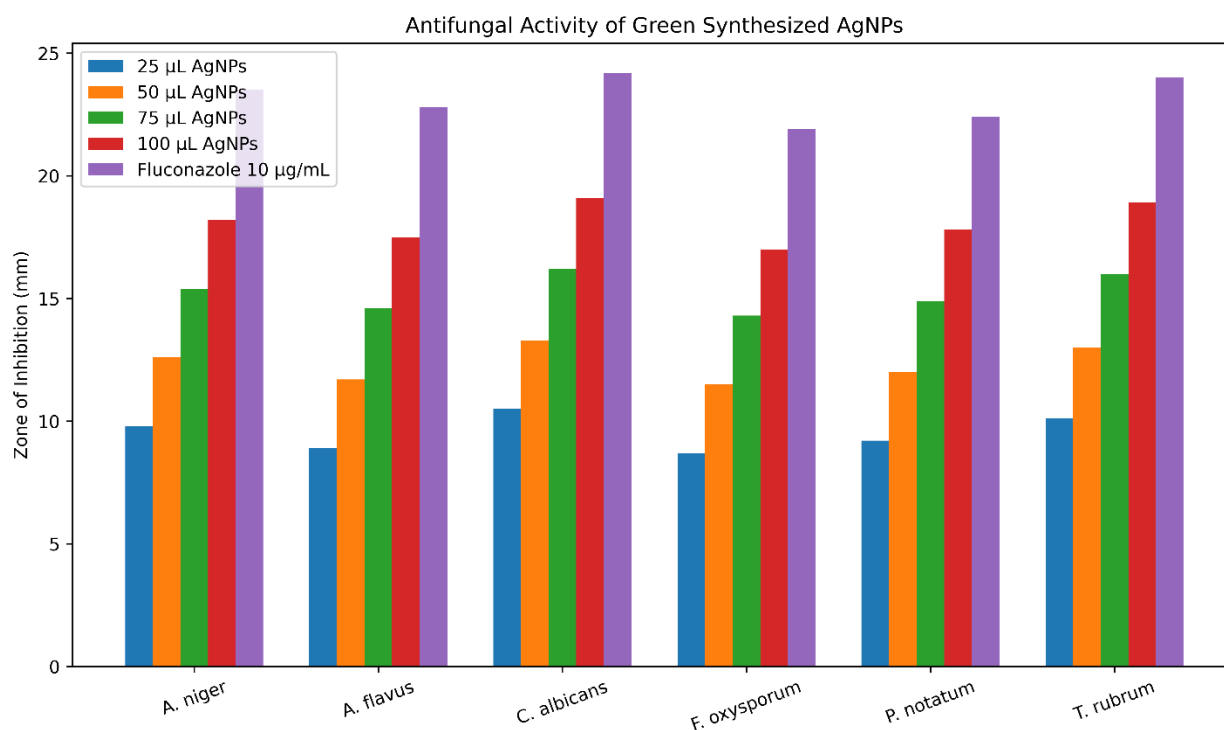


Figure 6. Antifungal activity of AgNPs synthesized from *Azadirachta indica*

3.5. Antiparasitic activity

Figure 7 presents the antiparasitic efficacy of *Azadirachta indica*-mediated AgNPs against a panel of medically important protozoan parasites at increasing concentrations (25–100 µL), alongside a standard reference drug (metronidazole, 10 µg/mL). Overall, the AgNPs exhibited a clear and

consistent dose-dependent increase in antiparasitic activity across all tested organisms. At the lowest tested concentration (25 μL), inhibition values ranged from $36.9 \pm 0.4\%$ to $43.0 \pm 0.5\%$, indicating a moderate baseline antiparasitic effect. As the concentration increased to 50 μL and 75 μL , a progressive enhancement in activity was observed, with inhibition reaching approximately 50–57% and 62–69%, respectively. The highest tested concentration (100 μL) produced the strongest antiparasitic response, with inhibition values between $74.1 \pm 0.6\%$ and $80.2 \pm 0.4\%$. Among the tested parasites, *Giardia lamblia* demonstrated the highest susceptibility ($80.2 \pm 0.4\%$ at 100 μL), followed closely by *Leishmania major* ($78.6 \pm 0.5\%$) and *Entamoeba histolytica* ($77.5 \pm 0.5\%$). In contrast, *Trypanosoma cruzi* showed comparatively lower sensitivity ($74.1 \pm 0.6\%$), suggesting a relatively higher resistance to nanoparticle-mediated stress. When compared with metronidazole, which exhibited inhibition values ranging from 88.7% to 93.0%, the AgNPs demonstrated slightly lower but still substantial antiparasitic activity, confirming their strong biological potential.

The results clearly demonstrate that AgNPs synthesized using *Azadirachta indica* possess significant broad-spectrum antiparasitic activity, which increases in a concentration-dependent manner (Kumari et al., 2026). This behavior is consistent with the typical pharmacodynamic response of nanoparticle-based antimicrobial systems, where higher particle availability enhances parasite–nanoparticle interactions. The antiparasitic mechanism of AgNPs is likely multifactorial. One of the primary modes of action involves direct interaction with parasite cell membranes, leading to increased permeability, structural damage, and eventual lysis. Due to their nanoscale size, AgNPs can easily adhere to and penetrate biological membranes, disrupting membrane integrity and cellular homeostasis (Kamalakaran et al., 2016). In addition, AgNPs are well known to induce the generation of reactive oxygen species (ROS), which results in oxidative stress. Excess ROS can damage lipids, proteins, and nucleic acids, ultimately leading to mitochondrial dysfunction and apoptosis-like cell death in protozoan parasites (Lateef et al., 2019). Furthermore, silver ions released from nanoparticles can interact with thiol (-SH) groups of essential enzymes,

thereby inhibiting critical metabolic pathways. The observed variation in susceptibility among parasites may be attributed to structural and biochemical differences (Lacey et al.,1989) . For instance, *Giardia lamblia* and *Leishmania major* showed higher sensitivity, which may be due to their relatively less complex cellular defense systems and higher membrane permeability. Conversely, *Trypanosoma cruzi* exhibited lower susceptibility, potentially due to more robust antioxidant defense mechanisms, complex surface glycoproteins, and enhanced cellular repair pathways that reduce nanoparticle-induced damage (Xie et al., 2022). Although the standard drug metronidazole demonstrated superior inhibitory activity, the AgNPs still showed considerable efficacy. Importantly, unlike conventional single-target drugs, AgNPs exert multi-target effects, reducing the likelihood of resistance development. This is particularly significant given the increasing prevalence of drug-resistant protozoan strains worldwide.

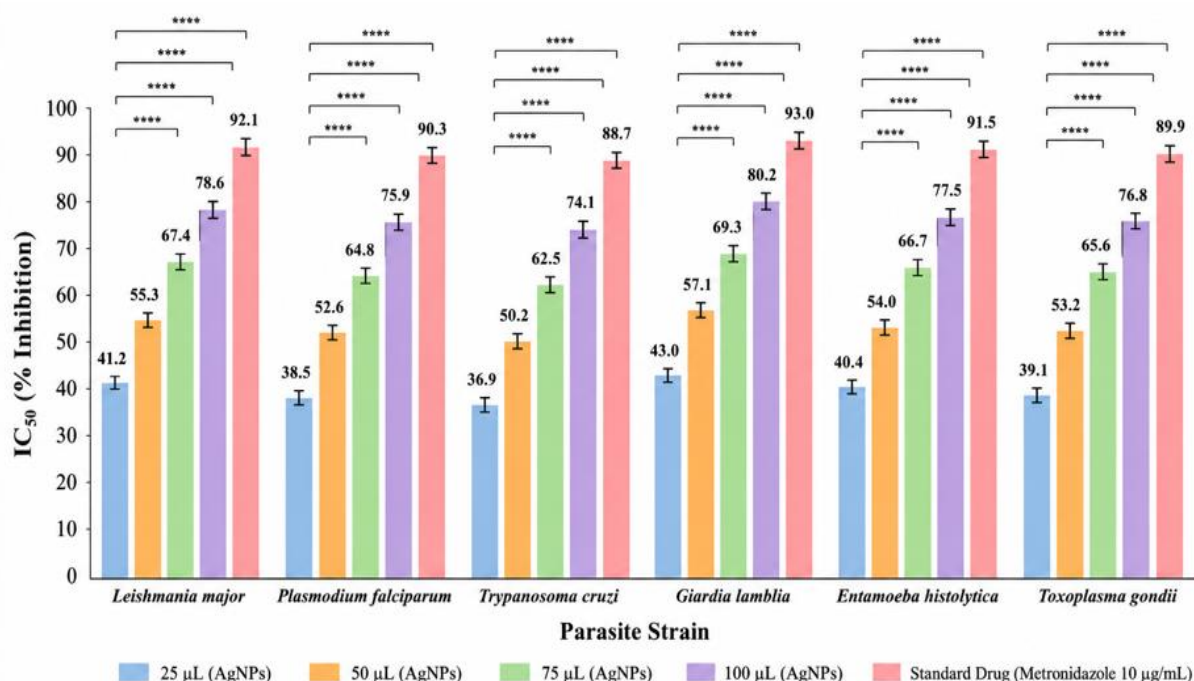


Figure 7. Antiparasitic Activity of bio-inspired AgNPs.

3.6. Biocompatibility assay

The biocompatibility profile of *Azadirachta indica*-mediated AgNPs demonstrated a concentration-dependent reduction in cell viability and a corresponding increase in hemolytic activity. At the lowest tested concentration (25 μ L), AgNPs exhibited high compatibility with mammalian cells, maintaining $92.4 \pm 0.5\%$ cell viability, with minimal hemolysis ($3.1 \pm 0.3\%$), indicating a non-cytotoxic nature. As the concentration increased, a gradual decline in cell viability was observed, reaching $79.2 \pm 0.6\%$ at 100 μ L, accompanied by a slight increase in hemolysis ($8.5 \pm 0.5\%$). Despite this reduction, the overall cytotoxicity remained within an acceptable range, suggesting that the nanoparticles retain moderate biocompatibility even at higher doses. The untreated control group showed normal cell viability (100%) and minimal hemolysis ($1.2 \pm 0.2\%$), confirming that observed effects were solely due to nanoparticle exposure. The biocompatibility results indicate that *Azadirachta indica*-mediated AgNPs exhibit a favorable safety profile at lower concentrations, making them suitable for biomedical applications. The relatively high cell viability at 25–50 μ L suggests that plant-capped nanoparticles possess reduced cytotoxicity due to the presence of bioactive phytochemicals acting as stabilizing and bioprotective agents. The observed dose-dependent cytotoxicity at higher concentrations can be attributed to increased cellular uptake of nanoparticles, leading to enhanced generation of reactive oxygen species (ROS), mitochondrial stress, and membrane disruption. Silver ions released from AgNPs may also interact with thiol-containing proteins, affecting cellular metabolic pathways. All these results are tabulated in Table 2.

Hemolysis results further confirm that AgNPs remain blood-compatible at lower doses, as values below 5% are generally considered safe for biomedical use (Loganathan et al, 2024). The slight increase in hemolysis at higher concentrations may result from direct interaction of nanoparticles with erythrocyte membranes, causing mild membrane destabilization. Importantly, despite moderate cytotoxicity at elevated concentrations, the AgNPs still demonstrate a therapeutically acceptable safety window, especially when compared to conventional antimicrobial agents that

DOI: <http://doi.org/10.5281/zenodo.20795632>

often exhibit higher systemic toxicity (Chahardoli et al., 2025). The phytochemical coating from *Azadirachta indica* likely plays a key role in reducing toxicity by improving nanoparticle stability and limiting uncontrolled silver ion release.

Table 2. In vitro biocompatibility of *Azadirachta indica*-mediated AgNPs

Concentration of AgNPs	Cell Viability		Cytotoxicity Level	Concentration of AgNPs
	(L929 / HeLa cells, %)	Hemolysis (%)		
25 μ L	92.4 \pm 0.5	3.1 \pm 0.3	Non-cytotoxic	25 μ L
50 μ L	88.7 \pm 0.6	4.8 \pm 0.4	Low cytotoxicity	50 μ L
75 μ L	83.5 \pm 0.5	6.2 \pm 0.5	Mild cytotoxicity	75 μ L
100 μ L	79.2 \pm 0.6	8.5 \pm 0.5	Moderate cytotoxicity	100 μ L
Control (untreated cells)	100 \pm 0.0	1.2 \pm 0.2	Non-toxic baseline	Control (untreated cells)

4. Conclusion

This study successfully demonstrated an eco-friendly and cost-effective synthesis of AgNPs Using *Azadirachta indica* leaf extract. The phytochemicals present in the plant extract acted efficiently as both reducing and stabilizing agents, leading to the formation of stable, crystalline, and predominantly spherical nanoparticles, as confirmed by UV–Vis spectroscopy, FTIR, XRD, and SEM analyses. The biosynthesized AgNPs exhibited strong and broad-spectrum antibacterial activity against both Gram-positive and Gram-negative bacteria, along with significant antifungal effects against clinically relevant fungal pathogens. Furthermore, the nanoparticles showed promising antiparasitic activity against protozoan parasites in a concentration-dependent manner, indicating their potential as alternative therapeutic agents. Importantly, biocompatibility studies revealed that the synthesized AgNPs maintain good cell viability and low hemolytic activity at lower

James et al - 2026

3007-2387

3007-2379

DOI: <http://doi.org/10.5281/zenodo.20795632>

concentrations, suggesting their suitability for biomedical use. Although a mild increase in cytotoxicity was observed at higher doses, the overall safety profile remained acceptable. In conclusion, *Azadirachta indica*-mediated AgNPs offer a sustainable nanotechnological approach with potent antimicrobial, antifungal, and antiparasitic properties combined with favorable biocompatibility. These findings support their potential application in future biomedical, pharmaceutical, and therapeutic developments, warranting further in vivo and clinical investigations.

Supplementary Information

Not applicable.

Acknowledgments

Not applicable.

Funding

Not applicable.

Data Availability

Data is made available on the request.

Competing interest

There are no competing interests among the authors.

Ethical responsibilities of authors

All authors have read and agreed to the final version of this paper. The manuscript has not been submitted to any other journal, nor is it under consideration. All the data and results produced have been prepared in this study.

Ethics approval

Not applicable.

Authors Contributions

Sana Habib contributed to the experimental design, data collection, and initial drafting of the manuscript. Muhammad Usman Tariq assisted in data analysis and interpretation of results and critically revised the manuscript for important intellectual content. Hidayat Ullah Farooqi supported the laboratory work, including sample preparation and experimental validation. Nasreen Ashraf* served as the corresponding author and supervised the overall research work, contributed to conceptualization, methodological guidance, and final approval of the manuscript. Muhammad Sabir Hussain contributed to statistical analysis, visualization of data, and manuscript editing. All authors reviewed and approved the final version of the manuscript.

Reference

- Malik, S., Muhammad, K., & Waheed, Y. (2023). Nanotechnology: a revolution in modern industry. *Molecules*, *28*(2), 661.
- Bamal, D., Singh, A., Chaudhary, G., Kumar, M., Singh, M., Rani, N., ... & Sehrawat, A. R. (2021). Silver nanoparticles biosynthesis, characterization, antimicrobial activities, applications, cytotoxicity and safety issues: An updated review. *Nanomaterials*, *11*(8), 2086.
- Burduşel, A. C., Gherasim, O., Grumezescu, A. M., Mogoantă, L., Fica, A., & Andronescu, E. (2018). Biomedical applications of silver nanoparticles: an up-to-date overview. *Nanomaterials*, *8*(9), 681.
- Jain, K., Takuli, A., Gupta, T. K., & Gupta, D. (2024). Rethinking nanoparticle synthesis: a sustainable approach vs. traditional methods. *Chemistry—An Asian Journal*, *19*(21), e202400701.
- Salem, S. S. (2023). A mini review on green nanotechnology and its development in biological effects. *Archives of Microbiology*, *205*(4), 128.
- Mutukwa, D., Taziwa, R. T., & Khotseng, L. (2024). A review of plant-mediated ZnO nanoparticles for photodegradation and antibacterial applications. *Nanomaterials*, *14*(14), 1182.
- Alamgir, A. N. M. (2017). *Therapeutic use of medicinal plants and their extracts: volume 1* (Vol. 73). Cham: Springer.
- Manojkumar, K., Sivaramakrishna, A., & Vijayakrishna, K. (2016). A short review on stable metal nanoparticles using ionic liquids, supported ionic liquids, and poly (ionic liquids). *Journal of Nanoparticle Research*, *18*(4), 103.
- Mshelmbula, B. P., Odozi, E. B., Wahedi, J. A., Ikhajagbe, B., & Anoliefo, G. O. (2025). Exploring Neem (*Azadirachta indica*): A Comprehensive Review of Its Uses and Advanced Breeding Techniques. *Biodiversity and Genetic Improvement of Medicinal and Aromatic Plants II*, 117-132.

- Alzohairy, M. A. (2016). Therapeutics role of Azadirachta indica (Neem) and their active constituents in diseases prevention and treatment. *Evidence-Based Complementary and Alternative Medicine*, 2016(1), 7382506.
- Roy, A., Bulut, O., Some, S., Mandal, A. K., & Yilmaz, M. D. (2019). Green synthesis of silver nanoparticles: biomolecule-nanoparticle organizations targeting antimicrobial activity. *RSC advances*, 9(5), 2673-2702.
- Melkamu, W. W., & Bitew, L. T. (2021). Green synthesis of silver nanoparticles using Hagenia abyssinica (Bruce) JF Gmel plant leaf extract and their antibacterial and anti-oxidant activities. *Helijon*, 7(11).
- Zuhrotun, A., Oktaviani, D. J., & Hasanah, A. N. (2023). Biosynthesis of gold and silver nanoparticles using phytochemical compounds. *Molecules*, 28(7), 3240.
- Kaur, H., Kumar, S., & Bouzid, G. (2024). Exploring the role of different phytochemicals on the morphological variations of metal and metal oxide nanomaterials for biomedical application. *Interactions*, 245(1), 234.
- Joudeh, N., & Linke, D. (2022). Nanoparticle classification, physicochemical properties, characterization, and applications: a comprehensive review for biologists. *Journal of nanobiotechnology*, 20(1), 262.
- Patel, R. R., Singh, S. K., & Singh, M. (2023). Green synthesis of silver nanoparticles: methods, biological applications, delivery and toxicity. *Materials Advances*, 4(8), 1831-1849.
- Vanlalveni, C., Lallianrawna, S., Biswas, A., Selvaraj, M., Changmai, B., & Rokhum, S. L. (2021). Green synthesis of silver nanoparticles using plant extracts and their antimicrobial activities: A review of recent literature. *RSC advances*, 11(5), 2804-2837.
- Mohan, A., Rajendran, S., & Palani, N. (2025). Sustainable synthesis of iron oxide nanoparticles using phytochemicals: mechanisms, functionalization strategies, applications and future perspectives. *Material Sci & Eng*, 9(2), 36-54.
- Tashi, T., Gupta, N. V., & Mbuya, V. B. (2016). Silver nanoparticles: Synthesis, mechanism of antimicrobial action, characterization, medical applications, and toxicity effects. *J. Chem. Pharm. Res*, 8(2), 526-537.
- Kumar, R., Sharma, S., & Devi, L. (2018). Investigation of total phenolic, flavonoid contents and antioxidant activity from extracts of Azadirachta indica of Bundelkhand Region. *Int. J. Life. Sci. Scienti. Res. eISSN*, 2455(1716), 1716.
- Poopathi, S., De Britto, L. J., Praba, V. L., Mani, C., & Praveen, M. (2015). Synthesis of silver nanoparticles from Azadirachta indica—a most effective method for mosquito control. *Environmental Science and Pollution Research*, 22(4), 2956-2963.
- Zhang, X. F., Liu, Z. G., Shen, W., & Gurunathan, S. (2016). Silver nanoparticles: synthesis, characterization, properties, applications, and therapeutic approaches. *International journal of molecular sciences*, 17(9), 1534.

- Tamboli, D. P., & Lee, D. S. (2013). Mechanistic antimicrobial approach of extracellularly synthesized silver nanoparticles against gram positive and gram negative bacteria. *Journal of hazardous materials*, 260, 878-884.
- Ahmed, M., Marrez, D. A., Mohamed Abdelmoeen, N., Abdelmoneem Mahmoud, E., Ali, M. A. S., Decsi, K., & Tóth, Z. (2023). Studying the antioxidant and the antimicrobial activities of leaf successive extracts compared to the green-chemically synthesized silver nanoparticles and the crude aqueous extract from *Azadirachta indica*. *Processes*, 11(6), 1644.
- Kummara, S., Patil, M. B., & Uriah, T. (2016). Synthesis, characterization, biocompatible and anticancer activity of green and chemically synthesized silver nanoparticles—a comparative study. *Biomedicine & Pharmacotherapy*, 84, 10-21.
- Saleem, S., Muhammad, G., Hussain, M. A., & Bukhari, S. N. A. (2018). A comprehensive review of phytochemical profile, bioactives for pharmaceuticals, and pharmacological attributes of *Azadirachta indica*. *Phytotherapy research*, 32(7), 1241-1272.
- Sidhu, A. K., Verma, N., & Kaushal, P. (2022). Role of biogenic capping agents in the synthesis of metallic nanoparticles and evaluation of their therapeutic potential. *Frontiers in Nanotechnology*, 3, 801620.
- Al-Arnoot, S., Abdullah, Q. Y., Al-Maqtari, M. A., Ibrahim, H. M., Al-Shamahy, H. A., Salah, E. M., ... & Al-Akhali, B. (2025). Multitarget antimicrobial mechanisms of plant extracts: A review of harnessing phytochemicals against drug-resistant pathogens. *Sana'a University Journal of Medicine and Health Sciences*, 19(4), 292-309.
- Shripad, T. S., & Asmita, R. S. (2025). Green Synthesis of Metal Nanoparticles Using Microbial and Plant Extracts for Biomedical Applications. *International Journal of Research & Technology*, 13(3), 726-735.
- Lorent, J. H., Quetin-Leclercq, J., & Mingeot-Leclercq, M. P. (2014). The amphiphilic nature of saponins and their effects on artificial and biological membranes and potential consequences for red blood and cancer cells. *Organic & biomolecular chemistry*, 12(44), 8803-8822.
- Hashem, A. H., Saied, E., Amin, B. H., Alotibi, F. O., Al-Askar, A. A., Arishi, A. A., ... & Elbahnasawy, M. A. (2022). Antifungal activity of biosynthesized silver nanoparticles (AgNPs) against aspergilli causing aspergillosis: Ultrastructure Study. *Journal of functional biomaterials*, 13(4), 242.
- Chinnasamy, G., Chandrasekharan, S., Koh, T. W., & Bhatnagar, S. (2021). Synthesis, characterization, antibacterial and wound healing efficacy of silver nanoparticles from *Azadirachta indica*. *Frontiers in microbiology*, 12, 611560.
- Babatimehin, A. M., Ajayi, G. O., Ogunbamowo, O. E., El-Rayyes, A., Albedair, L. A., Alsuhaibani, A. M., & Ofudje, E. A. (2025). Synthesis of silver nanoparticles using *Azadirachta indica* leaf extracts for heavy metal sensing. *BioResources*, 20(2), 334.

- Aljazzar, S. O., Babatimehin, A. M., Ogunbamowo, O. E., Refat, M. S., Albedair, L. A., & Ofudje, E. A. (2026). Eco-friendly silver nanoparticles from neem extracts: a dual approach to heavy metal sensing and antimicrobial applications. *Bioresources and Bioprocessing*, *13*(1), 18.
- Kaur, H., Kumar, S., & Bouzid, G. (2024). Exploring the role of different phytochemicals on the morphological variations of metal and metal oxide nanomaterials for biomedical application. *Interactions*, *245*(1), 234.
- Jadhav, V., Bhagare, A., Ali, I. H., Dhayagude, A., Lokhande, D., Aher, J., ... & Dutta, M. (2022). Role of Moringa oleifera on green synthesis of metal/metal oxide nanomaterials. *Journal of Nanomaterials*, *2022*(1), 2147393.
- Chinnasamy, G., Chandrasekharan, S., Koh, T. W., & Bhatnagar, S. (2021). Synthesis, characterization, antibacterial and wound healing efficacy of silver nanoparticles from *Azadirachta indica*. *Frontiers in microbiology*, *12*, 611560.
- Ulaeto, S. B., Mathew, G. M., Pancrecius, J. K., Nair, J. B., Rajan, T. P. D., Maiti, K. K., & Pai, B. C. (2019). Biogenic Ag nanoparticles from neem extract: their structural evaluation and antimicrobial effects against *Pseudomonas nitroreducens* and *Aspergillus unguis* (NII 08123). *ACS Biomaterials Science & Engineering*, *6*(1), 235-245.
- Rana, A., Kumari, A., Chaudhary, A. K., Srivastava, R., Kamil, D., Vashishtha, P., & Sharma, S. N. (2023). An investigation of antimicrobial activity for plant pathogens by green-synthesized silver nanoparticles using *Azadirachta indica* and *Mangifera indica*. *Physchem*, *3*(1), 125-146.
- Ezeh, C. K., Eze, C. N., Dibua, M. U. E., & Emencheta, S. C. (2024). A review on *Azadirachta indica* (neem) plant mediated biosynthesis, characterisation and antimicrobial activity of silver nanoparticles. *International Journal of Biomedical Nanoscience and Nanotechnology*, *5*(1), 15-36.
- Ulaeto, S. B., Mathew, G. M., Pancrecius, J. K., Nair, J. B., Rajan, T. P. D., Maiti, K. K., & Pai, B. C. (2019). Biogenic Ag nanoparticles from neem extract: their structural evaluation and antimicrobial effects against *Pseudomonas nitroreducens* and *Aspergillus unguis* (NII 08123). *ACS Biomaterials Science & Engineering*, *6*(1), 235-245.
- Giri, V. A., Sastry, S. V. A. R., & Kapoor, A. (2025). Biomass-assisted green synthesis and characterization of silver nanoparticles using *Azadirachta indica*, *Ocimum basilicum*, and *Curcuma longa*: evaluation of antifungal potential. *Biomass Conversion and Biorefinery*, *15*(19), 26323-26337.
- Kumari, P., Sarker, S., Vimal, B., & Saini, V. P. (2026). Green silver nanoparticles as a potential control strategy against *Ichthyophthirius multifiliis*: Efficacy and toxicity evaluation in goldfish, *Carassius auratus*. *Acta Tropica*, 108112.
- Kamalakaran, S., Ananth, S., Murugan, K., Kovendan, K., Ramar, M., Arumugam, P., ... & Balachandar, V. (2016). Bio fabrication of silver nanoparticle from *Argemone mexicana* for the control of *Aedes albopictus* and their antimicrobial activity. *Current Pharmaceutical Biotechnology*, *17*(14), 1285-1294.

James et al - 2026

3007-2387

3007-2379

DOI: <http://doi.org/10.5281/zenodo.20795632>

- Lateef, A., Elegbede, J., Akinola, O., & Ajayi, V. (2019). Biomedical applications of green Synthesized-Metallic nanoparticles. *Rev*, *3*, 157-82.
- Lacey, E. (1989). Comparative biochemistry of parasites and its role in drug resistance-an investigation of species differences in tubulin. In *Comparative Biochemistry of Parasitic Helminths* (pp. 145-167). Dordrecht: Springer Netherlands.
- Xie, Y., Liang, H., Jiang, N., Liu, D., Zhang, N., Li, Q., ... & Chen, Q. (2022). Graphene quantum dots induce cascadic apoptosis via interaction with proteins associated with anti-oxidation after endocytosis by *Trypanosoma brucei*. *Frontiers in Immunology*, *13*, 1022050.
- Loganathan, S., Manimaran, K., Prakash, D. G., Rajaji, U., Bahajjaj, A. A. A., & Liu, T. Y. (2024). Synthesis of silver nanoparticles (AgNPs) using *Pterolobium hexapetalum* (Roth) Santapau & Wagh and its investigation of biological activities. *Biomass Conversion and Biorefinery*, *14*(23), 30201-30214.
- Chahardoli, A., Qalekhani, F., Hajmomeni, P., Shokoohinia, Y., & Fattahi, A. (2025). Enhanced hemocompatibility, antimicrobial and anti-inflammatory properties of biomolecules stabilized AgNPs with cytotoxic effects on cancer cells. *Scientific Reports*, *15*(1), 1186.